Multiatom resonant photoemission observed via secondary processes: Auger decay and x-ray fluorescence

E. Arenholz

Materials Sciences Division, Lawrence Berkeley National Laboratory, Berkeley, California 94720

A. W. Kay and C. S. Fadley

Materials Sciences Division, Lawrence Berkeley National Laboratory, Berkeley, California 94720
and Department of Physics, University of California-Davis, Davis, California 95616

M. M. Grush and T. A. Callcott

Department of Physics, University of Tennessee, Knoxville, Tennessee 37996

D. L. Ederer

Department of Physics, Tulane University, New Orleans, Louisiana 70118

C. Heske* and Z. Hussain

Advanced Light Source, Lawrence Berkeley National Laboratory, Berkeley, California 94720

We present experimental evidence that the newly discovered multiatom resonant photoemission effect can be observed via secondary decay processes of the primary core hole: *Auger electron emission*, from Fe_2O_3, where the O $KL_{23}L_{23}$ intensity is enhanced by 90% when $h\nu$ is tuned to the Fe L_3 edge, and *fluorescent x-ray emission*, from MnO, where the O $K\alpha$ fluorescence intensity shows an enhancement of more than 100% at the Mn L_3 edge when properly corrected for saturation and self-absorption effects.

Intra-atomic resonant photoemission is a well-known and powerful tool for electronic structure studies.[1] In this effect, the photoelectron intensity from a given core or valence level can be significantly enhanced when the photon energy is just sufficient to excite an electron from a deeper lying core level in the same atom up to a bound excited state. This excited state then decays immediately so as to assist in producing a free electron at the same energy as that directly photoexcited from the core or valence level at lower binding energy. This resonant process is simultaneous and coherent with the direct excitation of the photoelectron and it can lead to significant increases (or decreases) in intensity, often following the well-known Fano profile. It is, however, only very recently that a closely related interatomic effect, which has been termed multiatom resonant photoemission (MARPE) and appears to involve several hundred atoms in the vicinity of a given emitter, has been observed.[2] MARPE occurs in photoemission from a core level of one atom as the photon energy is tuned to a deeper lying core absorption edge of another species atom in the vicinity of the emitting atom. This interatomic resonance leads to a significant increase in the core photoemission intensity of the emitter as compared to excitation off resonance, with effects of up to 100% in peak height being seen in various transition-metal oxides and alloys.[2] For most cases studied to date, the resonant enhancements follow very closely the x-ray absorption coefficient of the material.[2] A newly developed theoretical model of MARPE (Ref. 3) is able to describe quantitatively both the overall amplitude and the shape of the resonant enhancements seen in O $1s$ emission from MnO. Such interatomic resonant photoemission effects should thus constitute a broadly useful new probe of near-neighbor atomic identities, bonding, and magnetism.[2]

Since the MARPE process results in an enhanced probability of forming a particular core hole on the emitting atom, it should also be possible to detect the effect via the secondary decay processes of this hole, specifically Auger electron emission and fluorescent soft-x-ray emission. Detection via secondary decay processes would serve two purposes: further verifying the nature of the effect as described in prior work[2,3] and broadening its potential applications via other detection schemes. To investigate these possibilities, we have studied the photon energy dependence of both the O KLL Auger intensity at the Fe $L_{3,2}$ edges in Fe_2O_3 and the O $K\alpha$ fluorescence radiation intensity at the Mn $L_{3,2}$ edges in MnO; both processes result from filling an initial O $1s$ hole.

Electron emission measurements were performed on beamline 9.3.2 of the Advanced Light Source (ALS).[4,5] Fluorescence experiments were carried out using the grating spectrometer on the ALS beamline 8.0.1.[6] Samples consisting of a Fe_2O_3 thin film[7] and a single crystal of MnO(001) were cleaned by appropriate annealing, in oxygen for Fe_2O_3 and in an ultrahigh vacuum for MnO. The sample temperature was ambient (≈ 300 K) for Fe_2O_3 in all measurements and for MnO during fluorescence experiments. Photoemission and partial electron yield measurements on MnO were performed at ≈ 600 K to prevent sample charging.[8] The angle of light incidence θ_{in} was 20° with respect to the Fe_2O_3 sample surface and the electrons were collected in normal emission [see inset in Fig. 1(a)]. An angle of 90° was maintained between the exciting x rays and the photoelectron/
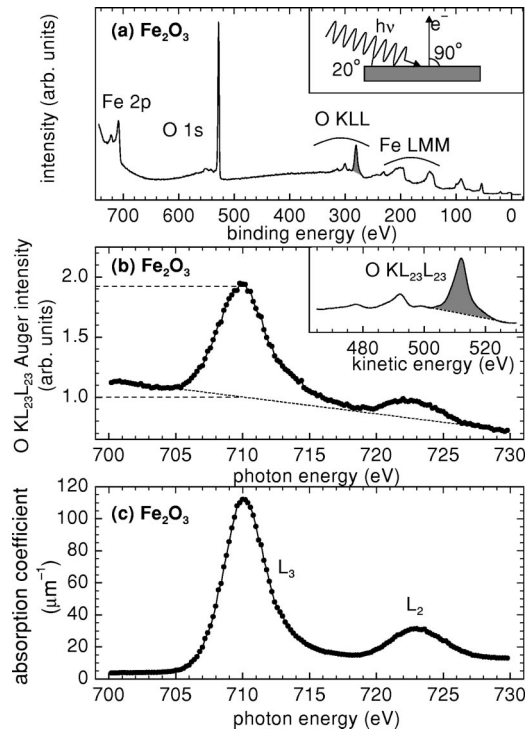
FIG. 1. (a) Photoemission/Auger spectrum of Fe_2O_3 taken at $h\nu = 800$ eV. The inset shows the experimental geometry. (b) O $KL_{23}L_{23}$ intensity—as indicated by the shaded area in the inset—as photon energy is scanned through the Fe $L_{3,2}$ edges. (c) X-ray absorption coefficient for Fe_2O_3 at the Fe $L_{3,2}$ edges as measured by partial electron yield.

FIG. 2. (a) Fluorescence spectrum of MnO recorded at $h\nu = 640$ eV. The inset shows the experimental geometry. (b) Energy dependence of the O $K\alpha$ fluorescence intensity as photon energy is scanned through the Mn $L_{3,2}$ edges for different angles of light incidence θ_{in}. (c) X-ray absorption coefficient of MnO at the Mn $L_{2,3}$ as measured by partial electron yield.

fluorescence detector for all experiments on MnO, with the incidence angle θ_{in} being systematically varied [see inset in Fig. 2(a)].

In Fe_2O_3, the Fe LMM Auger peaks appear at about 90 eV higher kinetic electron energy than the O KLL Auger [see Fig. 1(a)]. At the Fe $L_{3,2}$ edges, the intensities of these Fe Augers change significantly with photon energy, in turn leading to a changing inelastic background intensity below the O KLL Auger emission. Therefore, we have chosen to analyze the energy dependence of the most pronounced O KLL feature, i.e., the O $KL_{23}L_{23}$ peak, as corrected with a linear background [see inset in Fig. 1(b)], and the variation of this intensity with photon energy is shown in Fig. 1(b). For comparison, Fig. 1(c) shows the Fe_2O_3 absorption coefficient as measured with partial electron yield and an identical photon energy resolution. The O $KL_{23}L_{23}$ intensity clearly shows about 90% enhancement at the Fe L_3 edge as compared to the expected intensity without interatomic excitations, which is estimated by a linear interpolation of the Auger intensity below and above the Fe $L_{3,2}$ edges [dashed line in Fig. 1(b)]. This enhancement also is found to follow very closely the x-ray absorption coefficient in Fig. 1(c), in agreement with prior MARPE studies.[2] In a corresponding prior photoemission experiment on Fe_2O_3, the O $1s$ intensity is found to be enhanced by about 60% at the Fe L_3 edge.[2(a)] This difference in the overall magnitude of the effect will be discussed quantitatively later.

In the fluorescence measurements on MnO, the O $K\alpha$ x rays are well separated in energy from any Mn fluorescence feature, permitting us to determine the energy dependence of
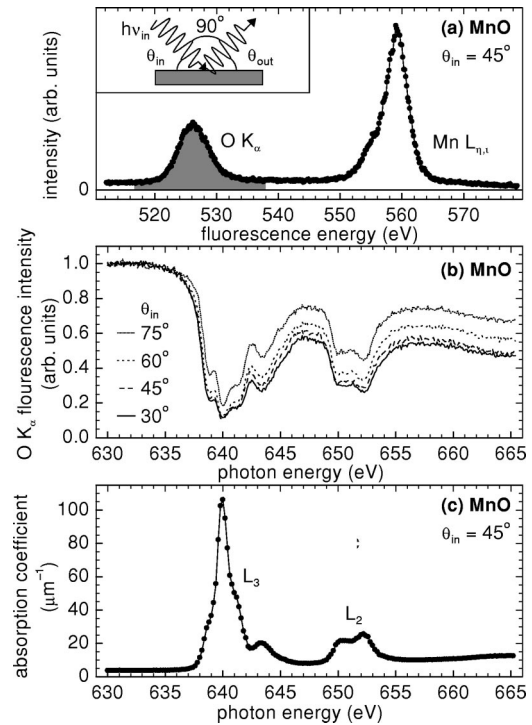
their intensity simply by considering an energy window of 20 eV centered at about 525 eV energy, as indicated by the shaded area in Fig. 2(a), and summing over the total area, minus a small background correction. The background is due to detector dark current (<0.01 counts/channel sec) and an equally significant amount of scattered light. The results of such energy scans for various experimental geometries are plotted in Fig. 2(b). For comparison, Fig. 2(c) shows the MnO absorption coefficient measured with partial electron yield. The O $K\alpha$ intensity shows minima when the excitation energy is tuned to the Mn $L_{3,2}$ edges instead of the maxima that might be expected based on the simplest interpretation of MARPE. However, these minima are due to well-known sample absorption effects for both the exciting and emitted fluorescence intensity, i.e., saturation and self-absorption phenomena.[9]

To correct for sample absorption, we consider a standard model: the intensity of the incoming x rays at a distance z from the surface is reduced by a factor $\exp[-\mu_{MnO}(h\nu_{in})z/\sin\theta_{in}]$ compared to the intensity at the sample surface, where $\mu_{MnO}(h\nu_{in})$ is the absorption coefficient of MnO at the photon energy of the incoming x rays $h\nu_{in}$. The probability that an O $1s$ hole is created in a layer of thickness dz is proportional to the O $1s$ cross section $\sigma_{O\,1s}$. The fluorescence yield $\epsilon_{O\,1s}$ then gives the probability that the O $1s$ hole decays via emission of O $K\alpha$ fluorescence radiation, and we assume that this is essentially constant over the small Mn $L_{3,2}$ region studied. On leaving the sample, the O $K\alpha$ radiation created at a distance z from the surface is then absorbed by the MnO according to

$\exp[-\mu_{MnO}(\mathrm{O}\ K\alpha)z/\sin\theta_{out}]$, where $\mu_{MnO}(\mathrm{O}\ K\alpha)$ is the absorption coefficient of MnO at the photon energy of the O $K\alpha$ radiation. Taking the absorption of the incoming and outgoing x rays into account and integrating over a semi-infinite sample finally allows us to calculate the expected photon energy dependence of the fluorescence intensity $I(\mathrm{O}\ K\alpha)$ at the detector:

$$I(\mathrm{O}\ K\alpha)\propto I_0(h\nu_{in})\sigma_{\mathrm{O}\ 1s}\epsilon_{\mathrm{O}\ 1s}[\mu_{MnO}(h\nu_{in})/\sin\theta_{in}$$
$$+\mu_{MnO}(\mathrm{O}\ K\alpha)/\sin\theta_{out}]^{-1}$$

.

As numerical inputs, we have used the experimentally determined Mn $L_{3,2}$ absorption coefficient [see Fig. 2(c)] and calibrated it to absolute units by matching the experimental data well below and above the Mn $L_{3,2}$ edges to the results of a standard calculation of x-ray absorption coefficients.[10] As an initial reference calculation, we made the assumption that the O $1s$ cross section $\sigma_{\mathrm{O}\ 1s}$ is constant over the entire energy range, i.e., resonant interatomic effects were neglected. The results are shown as the dashed curves in Fig. 3(a), where they are compared to our experimental results (solid curves). The experimental curves in Fig. 3(a) were obtained by broadening the actual experimental data shown in Fig. 2(b) with a Gaussian of 0.6-eV width in order to permit direct comparison with the calculated curves that are based on measurements of the x-ray absorption coefficient with lower resolution. Although the main features around the Mn $L_{3,2}$ edges and their variation with the angle of light incidence and exit are described correctly, there are significant percentage deviations between experiment and this nonresonant calculation. We attribute these differences to interatomic resonance effects on the O $1s$ cross section, and we can now estimate them simply by taking the ratio of the experimental data to the calculated curves, with both normalized to unity at an energy well below the resonance. The results are shown in Fig. 3(b) by solid lines. For all four geometries, we see clear and essentially identical curves indicating that the O $1s$ cross section as detected with O $K\alpha$ fluorescence radiation is enhanced at the Mn $L_{3,2}$ edges, and furthermore that it follows the shape of the Mn $L_{3,2}$ absorption coefficient, in agreement with prior photoemission results for MnO. Even though the shapes of the raw O $K\alpha$ intensity curves change appreciably with θ_{in} [cf. Fig. 3(a)], our analysis to derive the MARPE influence is fully self-consistent in yielding essentially the same curves for all four angles.

The peak amplitude of the resonant enhancement at the Mn L_3 edge varies between 100% and 140% using fluorescence detection whereas for photoelectron detection it changes between 36% and 50% with the angle of light incidence.[2] This difference has its origin in the different probing depths of photoelectrons and fluorescent x rays. It can be estimated quantitatively by considering the attenuation lengths of the incoming x rays, the emitted photoelectrons, and the fluorescence radiation, as well as the sensing length of the MARPE effect. For excitation at the Mn L_3 edge the attenuation length of the incoming radiation is approximately 95 Å [see Fig. 2(c)]. The O $1s$ photoelectrons have a kinetic energy of ≈110 eV and with that an inelastic
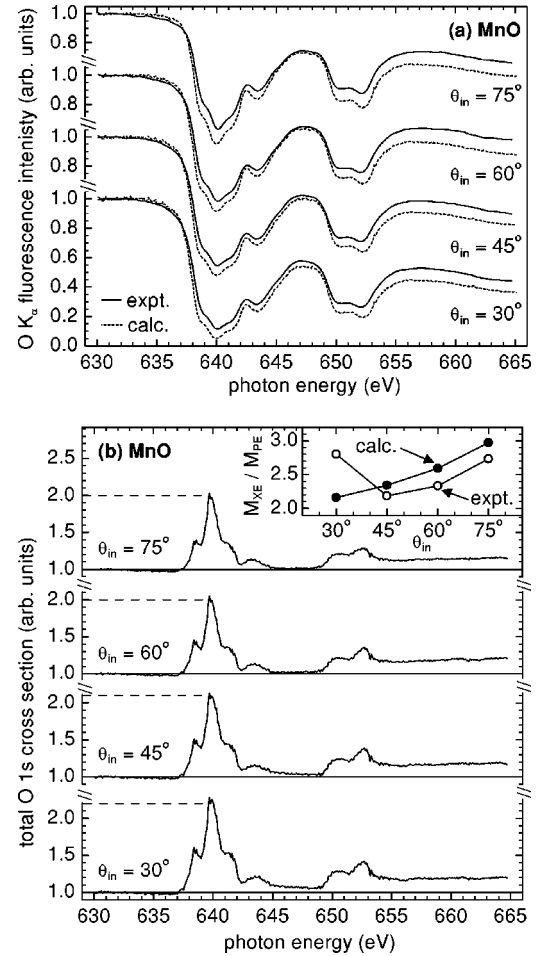

FIG. 3. (a) Experimental (solid curves) and calculated (dashed curves) energy dependence of the O $K\alpha$ fluorescence intensity at the Mn $L_{3,2}$ edges for different angles of light incidence θ_{in}. (b) O $1s$ cross section in MnO, including interatomic resonance effects, as derived from the two sets of curves shown in (a). The inset shows the experimental (open symbols) and calculated (filled symbols) ratio between the resonant enhancement at the Mn L_3 edge as detected via O $K\alpha$ fluorescence radiation M_{XE} and via O $1s$ photoelectrons M_{PE} for different experimental geometries. For details, see the text.

mean free path of about 7 Å in MnO.[11] By contrast, the attenuation length of the fluorescent O $K\alpha$ radiation is about 4500 Å in MnO.[10] As to the sensing length, theoretical calculations of the MARPE effect in MnO (Ref. 3) show good quantitative agreement with the experimental results[2(a)] if contributions from resonating Mn atoms up to a distance of 22 Å from the O emitter are taken into account. We have also recently experimentally determined an effective exponential sensing length in photoemission experiments on Cr/Fe overlayer samples,[2(b)] and this also yields approximately 20 Å. We thus estimate the contribution of a Mn atom at a distance r from a given O emitter to the resonant enhancement in the O $1s$ photoemission intensity by an exponential of the form $\exp(-r/r_0)$, with $r_0=20$ Å. By summing over these contributions and taking the attenuation of the incoming radiation and outgoing particles into account, we can thus calculate the ratio between the MARPE enhancements at the Mn L_3 edge as seen by both detection methods M_{XE}/M_{PE}. The inset in Fig. 3(b) shows the experi-

mentally determined as well as the calculated ratio. The agreement between experiment and our simple model calculation is remarkably good for all experimental geometries, i.e., the difference in the observed resonant enhancement can indeed be attributed to the different probing depth of photoelectrons and fluorescent x rays.

An analogous calculation can be made for the Auger electron emission and photoemission experiments on Fe_2O_3. At the Fe L_3 edge the O $KL_{23}L_{23}$ Auger electrons have a significantly higher kinetic energy (≈ 510 eV) than the O $1s$ photoelectrons (≈ 180 eV) and therefore a larger inelastic mean free path (14 Å vs 7 Å , respectively).[11] The attenuation length of the incoming x rays is about 90 Å at the Fe L_3 edge as derived from the experimental x-ray absorption coefficient normalized to absolute units, as in the case of MnO. With these numbers, we find that the resonant enhancement should be about 1.2 times more pronounced using Auger electron detection as compared to photoelectron detection. Experimentally we find from three different measurements an enhancement of the O $KL_{23}L_{23}$ intensity of $(90\pm 20)\%$ and with that an increase that is 1.5 ± 0.3 times more pronounced, in reasonable agreement with the model.

In summary, we have shown experimentally that multi-atom resonant photoemission (MARPE) effects can also be observed via secondary decay processes of the core hole whose formation is enhanced, specifically Auger electron emission and fluorescent soft x-ray emission. These results confirm the original explanation of the effect,[2(a)] and also provide new methods for detecting it, with applications to bulk materials possible via x-ray detection. The observed enhancements are larger using secondary processes for detection than in the primary photoelectron emission, by as much as a factor of 2 for fluorescence detection. These differences can be attributed to the different probing depths of photoelectrons and Auger electrons of significantly different kinetic energies and of fluorescent photons.

*Present address: Experimentelle Physik II, Universität Würzburg, Am Hubland, D-97074 Würzburg, Germany.

[1] C.-O. Almbladh and L. Hedin, in *Handbook on Synchrotron Radiation*, edited by E. E. Koch (North-Holland, Amsterdam, 1983), Vol. 1; *Giant Resonances in Atoms, Molecules and Solids*, Vol. 151 of *NATO Advanced Study Institute Series B: Physics*, edited by J.P. Connerade (Plenum, New York, 1987); J.W. Allen, in *Synchrotron Radiation Research: Advances in Surface and Low Dimensional Science*, edited by R.F. Bachrach (Plenum, New York, 1992), Vol. 1, Chap. 8, and references therein.

[2] (a) A. Kay *et al.*, Science **281**, 679 (1998); (b) E. Arenholz, A. Kay, and C.S. Fadley (unpublished).

[3] F. J. Garcia de Abajo, C. S. Fadley, and M. A. Van Hove, Phys. Rev. Lett. **82**, 4126 (1999).

[4] Z. Hussain *et al.*, J. Electron Spectrosc. Relat. Phenom. **80**, 401 (1996).

[5] C. S. Fadley *et al.*, J. Electron Spectrosc. Relat. Phenom. **75**, 273 (1995).

[6] J. J. Jia *et al.*, Rev. Sci. Instrum. **66**, 1394 (1995).

[7] S. Thevuthasan *et al.*, Surf. Sci. **425**, 276 (1999).

[8] B. Hermsmeier *et al.*, Phys. Rev. B **42**, 11 895 (1990).

[9] J. Jaklevic *et al.*, Solid State Commun. **23**, 679 (1977); F. M. F. de Groot *et al.*, *ibid.* **92**, 991 (1994); G. Faigel and M. Tegze, Rep. Prog. Phys. **62**, 355 (1999).

[10] B. L. Henke, E. M. Gullikson, and J. C. Davis, At. Data Nucl. Data Tables **54**, 181 (1993); E. Gullikson, Center for X-ray Optics, Lawrence Berkeley National Laboratory, public access program available at www-cxro.lbl.gov

[11] C. J. Powell *et al.*, J. Electron Spectrosc. Relat. Phenom. **68**, 605 (1994).